Chapter 6

Bioconvective EMHD nanofluid flow past a stretching sheet *

6.1 Introduction

Carbon nanotubes (CNTs) are highly recognized for their diverse biomedical applications. Electromagnetohydrodynamics (EMHD) is the area that concerns the study of dynamics of electrically conducting fluids under the influence of the magnetic and electric fields. EMHD has raised quite an interest over the years due to its versatile application in geophysics, engineering, biomedical engineering, magnetic drug targeting and many others. The present study aims to numerically and statistically study the stratification effects of bioconvective EMHD flow past a stretching sheet using water-based CNT. The current study, with applications ranging from biomedical imaging, targeted drug delivery, and cancer therapy, provides a theoretical perspective that is beneficial in biomedical engineering. The mathematically modelled system of partial differential equations (PDEs) is then transmuted into a system of ordinary differential equations (ODEs) using apposite transformations which are then resolved numerically using *bvp*5*c* (MATLAB built-in function) algorithm. The impact of influential parameters on concentration, velocity, microbial concentration, temperature and physical quantities are illustrated with the aid of graphs and tables. Further, statistical techniques like correlation, the slope of linear regression, probable error and multiple linear regression are employed in scrutinizing the consequence of influential parameters on physical quantities. The main objectives of the current chapter are to:

*Published in: Heat Transfer (Wiley), 2021; 50(7); 6680-6702.

- Construct the mathematical model to study the EMHD bioconvective CNT nanofluid flow past a stretching sheet considering thermal, solutal, and motile density stratification effects.

- Provide theoretical knowledge on the consequence of pertinent parameters on flow profiles.

- Predict the formulae for drag coefficient and heat transfer rate using multiple linear regression.

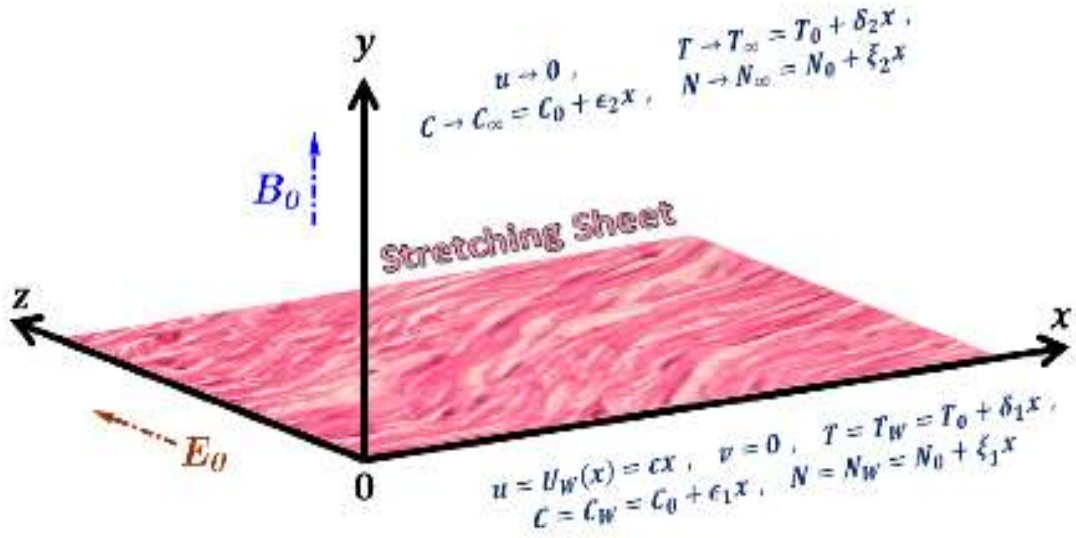

Figure 6.1: Geometrical Frame

6.2 Mathematical Frame

Consider a two-dimensional steady incompressible bioconvective flow over a lengthening sheet positioned along $x-$axis (see Figure 6.1) stretching with a velocity $U_W(x) = cx$. Water-based SWCNT nanofluid (containing microorganisms) occupies the region $y > 0$. A uniform electric field of strength E_0 and a uniform magnetic field of strength B_0 is applied normal to the fluid flow. Thermal, solutal and motile density stratification effects are incorporated. Further, viscous dissipation and chemical reaction effects are also considered.

Under these assumptions, the governing equations take the form (see Daniel et al., 2020; Daniel, Aziz, Ismail, & Salah, 2017a):

$$\frac{\partial u}{\partial x}+\frac{\partial v}{\partial y}=0 \tag{6.2.1}$$

$$u\frac{\partial u}{\partial x}+v\frac{\partial u}{\partial y}=\left(\frac{\mu_{nf}}{\rho_{nf}}\right)\frac{\partial^2 u}{\partial y^2}+\frac{\sigma_{nf}\ \left(E_0\ B_0-{B_0}^2\ u\right)}{\rho_{nf}} \tag{6.2.2}$$

$$u\frac{\partial T}{\partial x}+v\frac{\partial T}{\partial y}=\alpha_{nf}\frac{\partial^2 T}{\partial y^2}+\frac{\mu_{nf}}{(\rho C_p)_{nf}}\left(\frac{\partial u}{\partial y}\right)^2 \tag{6.2.3}$$

$$u\frac{\partial C}{\partial x}+v\frac{\partial C}{\partial y}=D_B\frac{\partial^2 C}{\partial y^2}-k_r\left(C-C_\infty\right) \tag{6.2.4}$$

$$u\frac{\partial N}{\partial x}+v\frac{\partial N}{\partial y}+\frac{bW_c}{C_W-C_0}\left(\frac{\partial}{\partial y}\left(N\frac{\partial C}{\partial y}\right)\right)=D_m\frac{\partial^2 N}{\partial y^2} \tag{6.2.5}$$

subject to the boundary conditions (Daniel et al., 2020, 2017a; Alsaedi et al., 2017):

$$\begin{gathered}u=U_W(x)=cx,\ v=0,\ T=T_W=T_0+\delta_1 x,\\ C=C_W=C_0+\epsilon_1 x,\ N=N_W=N_0+\xi_1 x \qquad \text{at } y=0\end{gathered}$$

$$\begin{gathered}u\to 0,\ T\to T_\infty=T_0+\delta_2 x,\\ C\to C_\infty=C_0+\epsilon_2 x,\ N\to N_\infty=N_0+\xi_2 x \qquad \text{as } y\to\infty\end{gathered}$$

Consider the following similarity transformations (see W. Khan & Pop, 2010; Alsaedi et al., 2017):

$$u=cxf\,'(\eta),\ v=-\sqrt{c\vartheta_f}f(\eta),\ \eta=y\sqrt{\frac{c}{\vartheta_f}},$$

$$\theta(\eta)=\frac{T-T_\infty}{T_W-T_0},\ \psi(\eta)=\frac{C-C_\infty}{C_W-C_0},\ \chi(\eta)=\frac{N-N_\infty}{N_W-N_0}$$

Employing the similarity transformations into Equations (6.2.1) – (6.2.5), we get:

$$f\,'''-A_1\ A_2\ \left\{\ (f\,')^2-f\ f\,''-\frac{A_5}{A_2}\ (M(\ E-f\,'))\ \right\}=0 \tag{6.2.6}$$

$$\theta\,''+\frac{A_3\ Pr}{A_4}\ f\ \theta\,'+\frac{Ec\ Pr}{A_1\ A_4}\ (f\,'')^2=0 \tag{6.2.7}$$

$$\psi\,''+Le\ f\ \psi\,'-Kr\ Le\ \psi=0 \tag{6.2.8}$$

$$\chi\,'' + Lb\ f\ \chi\,' - Pe\ \{\ (\ \chi + \Omega\ )\ \ \psi\,'' + \chi\,'\ \psi\,'\ \} = 0 \tag{6.2.9}$$

subject to the boundary conditions

$$f\,(0) = 0,\ \ f\,'(0) = 1,\ \ \theta\,(0) = 1 - s_1,\ \ \psi\,(0) = 1 - s_2,\ \ \chi\,(0) = 1 - s_3,$$
$$f\,'(\infty) \to 0,\ \ \theta\,(\infty) \to 0,\ \ \psi\,(\infty) \to 0,\ \ \chi\,(\infty) \to 0.$$

where the dimensionless parameters are given in appendix I.
The nanofluid models incorporated are (see Z. Iqbal, Azhar, & Maraj, 2017; Sreedevi & Reddy, 2019):

Effective Dynamic Viscosity : $\dfrac{\mu_{nf}}{\mu_f} = \dfrac{1}{(1-\phi)^{2.5}} = \dfrac{1}{A_1}$

Effective Density : $\dfrac{\rho_{nf}}{\rho_f} = (1-\phi) + \phi\left(\dfrac{\rho_{SWCNT}}{\rho_f}\right) = A_2$

Effective Specific Heat : $\dfrac{(\rho C_p)_{nf}}{(\rho C_p)_f} = (1-\phi) + \phi\left(\frac{(\rho C_p)_{SWCNT}}{(\rho C_p)_f}\right) = A_3$

Effective Thermal Conductivity : $\dfrac{k_{nf}}{k_f} = \dfrac{(1-\phi) + 2\phi\ \frac{k_{SWCNT}}{k_{SWCNT}-k_f}\ ln\left(\frac{k_{SWCNT}+k_f}{2k_f}\right)}{(1-\phi) + 2\phi\ \frac{k_f}{k_{SWCNT}-k_f}\ ln\left(\frac{k_{SWCNT}+k_f}{2k_f}\right)} = A_4$

Effective Electrical Conductivity : $\dfrac{\sigma_{nf}}{\sigma_f} = 1 + \dfrac{3\left(\frac{\sigma_{SWCNT}}{\sigma_f} - 1\right)\phi}{\left(\frac{\sigma_{SWCNT}}{\sigma_f} + 2\right) - \left(\frac{\sigma_{SWCNT}}{\sigma_f} - 1\right)\phi} = A_5$

The physical quantities are given by (see Z. Iqbal, Azhar, & Maraj, 2017; Daniel et al., 2020, 2017a; Alsaedi et al., 2017):

Local drag coefficient : $Cf_x = \dfrac{\tau_\omega}{\rho_f\ (U_W)^2} = \dfrac{\mu_{nf}\ \left.\frac{\partial u}{\partial y}\right|_{y=0}}{\rho_f\ (U_W)^2}$

$$\Rightarrow\ Cf_x\ Re_x^{1/2} = \frac{f\,''(0)}{A_1}$$

$$\text{Local Nusselt number} \quad : \quad Nu_x = \frac{x\ q_\omega}{k_f\ (T_W - T_0)} = \frac{-x\ k_{nf}\ \left.\frac{\partial T}{\partial y}\right|_{y=0}}{k_f\ (T_W - T_0)}$$

$$\Rightarrow\ Nu_x\ Re_x^{-\ 1/2} = -A_4\ \theta\,'(0)$$

$$\text{Local Sherwood number} \quad : \quad Sh_x = \frac{x\ q_m}{D_B\ (C_W - C_0)} = \frac{-x\ D_B\ \left.\frac{\partial C}{\partial y}\right|_{y=0}}{D_B\ (C_W - C_0)}$$

$$\Rightarrow\ Sh_x\ Re_x^{-\ 1/2} = -\ \psi\,'(0)$$

$$\text{Local motile density number} \quad : \quad Nn_x = \frac{x\ q_n}{D_m\ (N_W - N_0)} = \frac{-x\ D_m\ \left.\frac{\partial N}{\partial y}\right|_{y=0}}{D_m\ (N_W - N_0)}$$

$$\Rightarrow\ Nn_x\ Re_x^{-\ 1/2} = -\ \chi\,'(0)$$

where $Re_x = \frac{xU_W}{\vartheta_f}$ is the local Reynold's number.

6.3 Numerical Frame & Validation

Equations (6.2.6) – (6.2.9) along with the boundary conditions are resolved numerically manoeuvring *bvp5c* solver, a MATLAB built-in function. For this, choose:

$$f = y_1,\ f\,' = y_2,\ f\,'' = y_3,\ \theta = y_4,\ \theta\,' = y_5,\ \psi = y_6,\ \psi\,' = y_7,\ \chi = y_8,\ \chi\,' = y_9$$

Accordingly, the system of first-order ODEs is given by:

$$y_1^{'} = y_2,\ y_2^{'} = y_3,\ y_3^{'} = A_1\ A_2\ \left\{\ (y_2)^2 - y_1\ y_3 - \tfrac{A_5}{A_2}\ (M\,(E - y_2))\ \right\}$$

$$y_4^{'} = y_5,\ y_5^{'} = -\tfrac{A_3\ Pr}{A_4}\ y_1\ y_5 - \tfrac{Ec\ Pr}{A_1\ A_4}\ (y_3)^2$$

$$y_6^{'} = y_7,\ y_7^{'} = Kr\ Le\ y_6 - Le\ y_1\ y_7$$

$$y_8^{'} = y_9,\ y_9^{'} = Pe\ \left\{\ (y_8\ + \Omega)\ y_7^{'} + y_9\ y_7\ \right\} - Lb\ y_1\ y_9.$$

with

$$y_1\,(0) = 0,\ \ y_2\,(0) = 1,\ \ y_4\,(0) = 1 - s_1,\ \ y_6\,(0) = 1 - s_2,\ \ y_8\,(0) = 1 - s_3,$$
$$y_2\,(\infty) \to 0,\ \ y_4\,(\infty) \to 0,\ \ y_6\,(\infty) \to 0,\ \ y_8\,(\infty) \to 0.$$

Validation of the current problem and accuracy of the code have been accounted for through a restrictive comparison of the present work with prior published works of W. A. Khan et al., 2010; Wang, 1989 (showcased in Table 6.1) and a commendable agreement is noted.

Table 6.1: Comparison of $Nu_x(Re_x)^{-1/2}$ for differing Pr values between the present study and the works of W. A. Khan et al., 2010; Wang, 1989 when $M = E = Kr = Ec = Le = Lb = Pe = \Omega = s_1 = s_2 = s_3 = 0$

Pr	$\mathbf{Nu_x(Re_x)^{-1/2}}$		
	W. A. Khan et al., 2010	**Wang, 1989**	**Present study**
0.7	0.4539	0.4539	0.4539
2	0.9113	0.9114	0.9114
7	1.8954	1.8954	1.8954
20	3.3539	3.3539	3.3539
70	6.4621	6.4622	6.4622

Table 6.2: Thermophysical properties of water and SWCNT

Property	**Water (base fluid)**	**SWCNT (nanoparticle)**
$\boldsymbol{\rho}$	997	2600
$\boldsymbol{C_p}$	4179	425
$\boldsymbol{k}$	0.613	6600
$\boldsymbol{\sigma}$	0.05	10^6

6.4 Results & Discussion

The consequence of various influential parameters on microbial concentration ($\chi(\eta)$), velocity ($f'(\eta)$), concentration ($\psi(\eta)$), and temperature ($\theta(\eta)$) profiles are illustrated via Figures 6.2 - 6.9 with Prandtl number and infinity fixed at 6.2 and 3, respectively. Thermophysical properties of SWCNT and water are showcased in Table 6.2.

Figure 6.2 describes the decreasing nature of when magnetic field parameter is increased meaning that the velocity drops when the magnetic field parameter is increased. Physically, it is associated with the generation of Lorentz force (a frictional force) which reduces the velocity. From Figure 6.3, it is observed that the velocity improves due to augmenting electric field parameter. Biologically, magnetic field and electric field parameters play a crucial role since these parameters are responsible for manipulating the transport of nanofluid to the desired location and also for improved biomedical imaging.

Figure 6.4 indicates that nanoparticle volume fraction (ϕ) enhances the temperature profile. This increase in temperature can be related to the improvement in the thermal conductivity of the nanofluid caused by larger nanoparticle occupancy. The analysis on the effect of ϕ on the temperature unveils that the nanofluid can be used for killing tumors or cancerous cells. The impact of Eckert number (Ec) is depicted in Figure 6.5. As Ec is amplified, the temperature profile enlarges. Physically, it is associated with the generation of friction forces between the fluid particles which increases the temperature profile. A decline in temperature is noted when the thermal stratification parameter (s_1) is increased (see Figure 6.6). Physically, the decrease in temperature is due to the decrease in the temperature difference between the surface and away from the surface caused by an increase in s_1.

A decline in concentration is noted (see Figure 6.7) when the chemical reaction parameter (Kr) is increased. Physical reason being that an increase in Kr consumes more nanoparticles and hence concentration decreases. Biologically, consumption of more nanoparticles is directly proportional to improved medication and biomedical imaging. A decline in concentration is noted (due to the decrease in the volumetric fraction between the surface and reference nanoparticles) when the solutal stratification parameter (s_2) is increased (see Figure 6.8). The variation of motile density stratification parameter (s_3) is given in Figure 6.9. A decline in microbial concentration is noted. Physically, an augmentation in s_3 decreases the concentration difference of microorganisms between the surface and away from the surface and hence microbial concentration decreases.

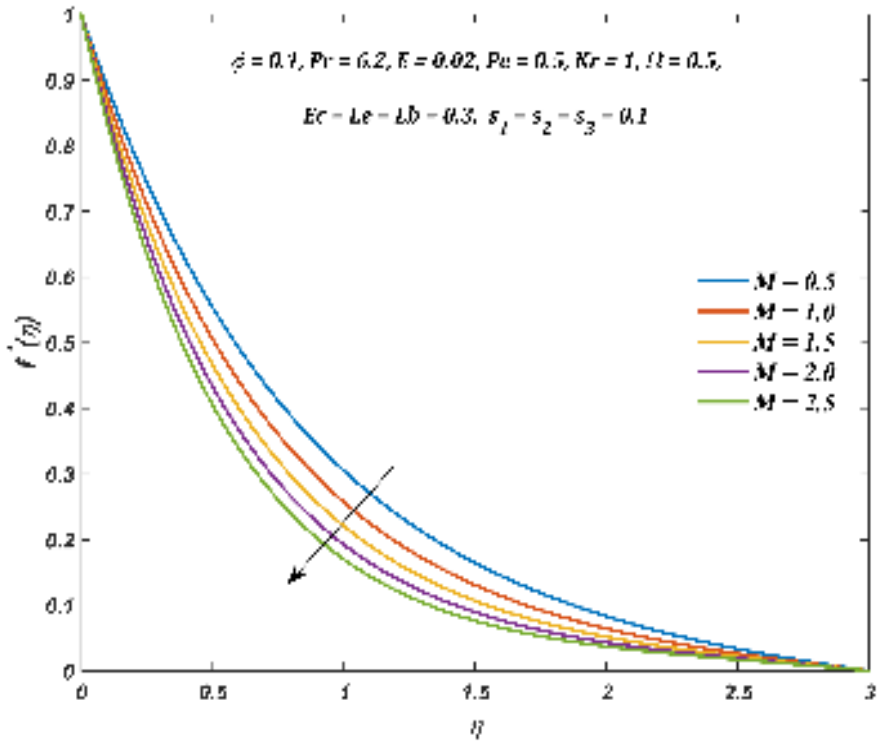

Figure 6.2: $f'(\eta)$ for differing M values

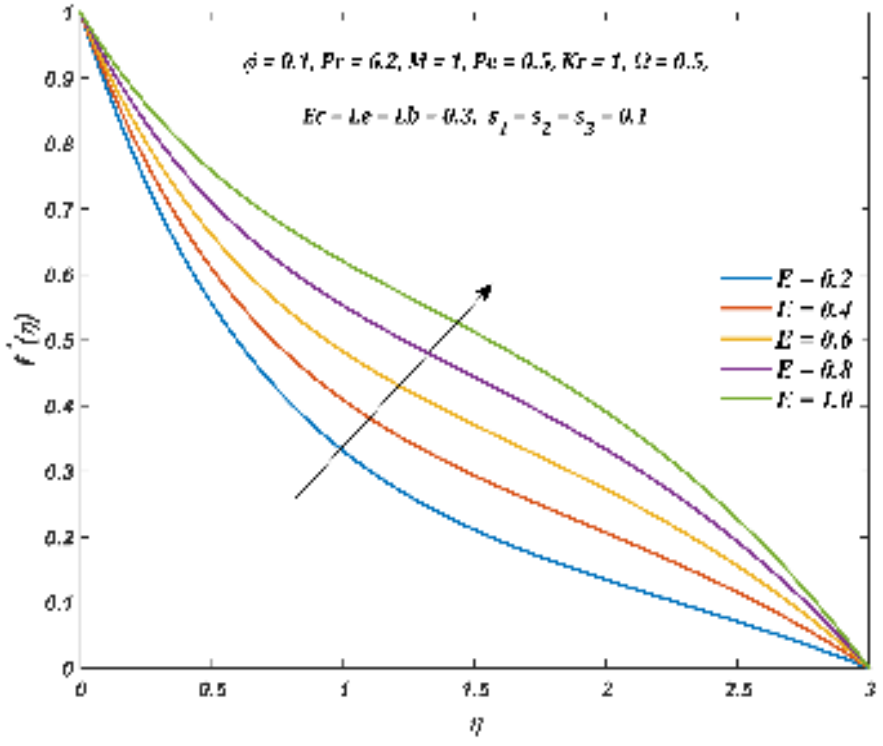

Figure 6.3: $f'(\eta)$ for differing E values

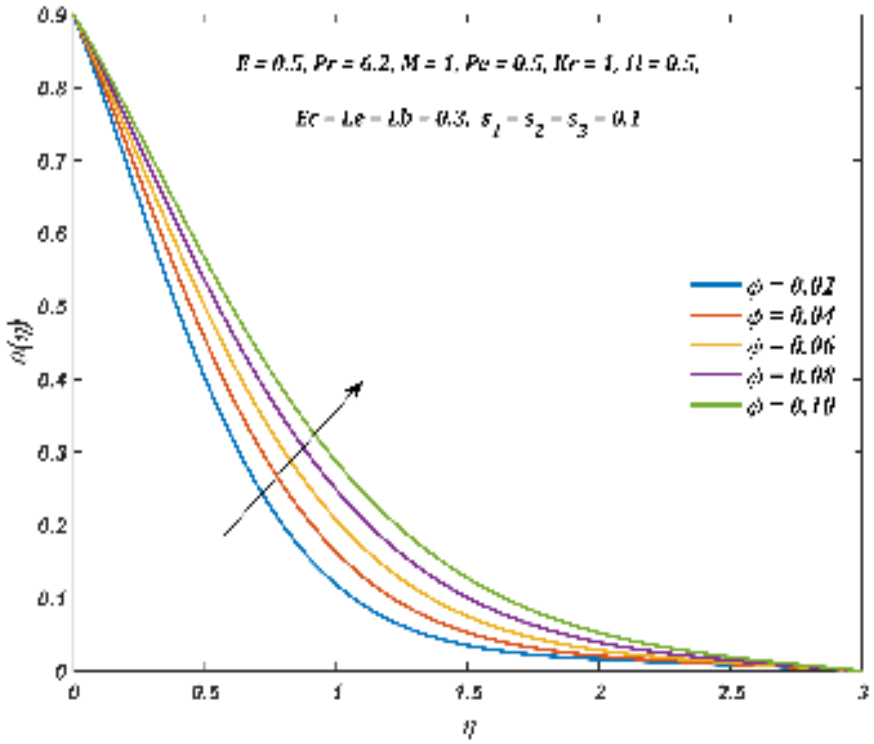

Figure 6.4: $\theta(\eta)$ for differing ϕ values

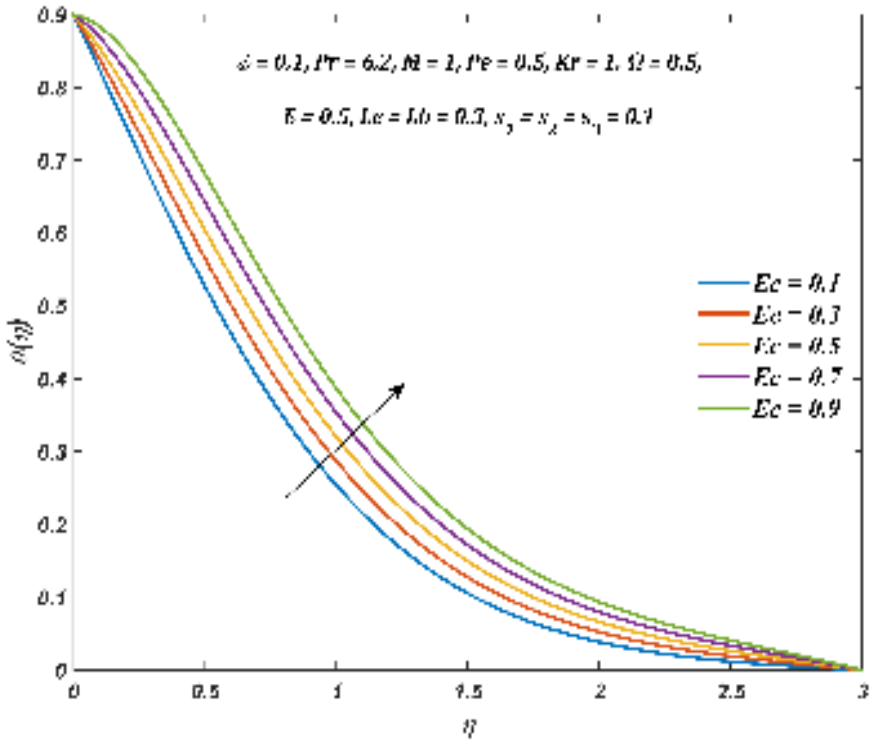

Figure 6.5: $\theta(\eta)$ for differing Ec values

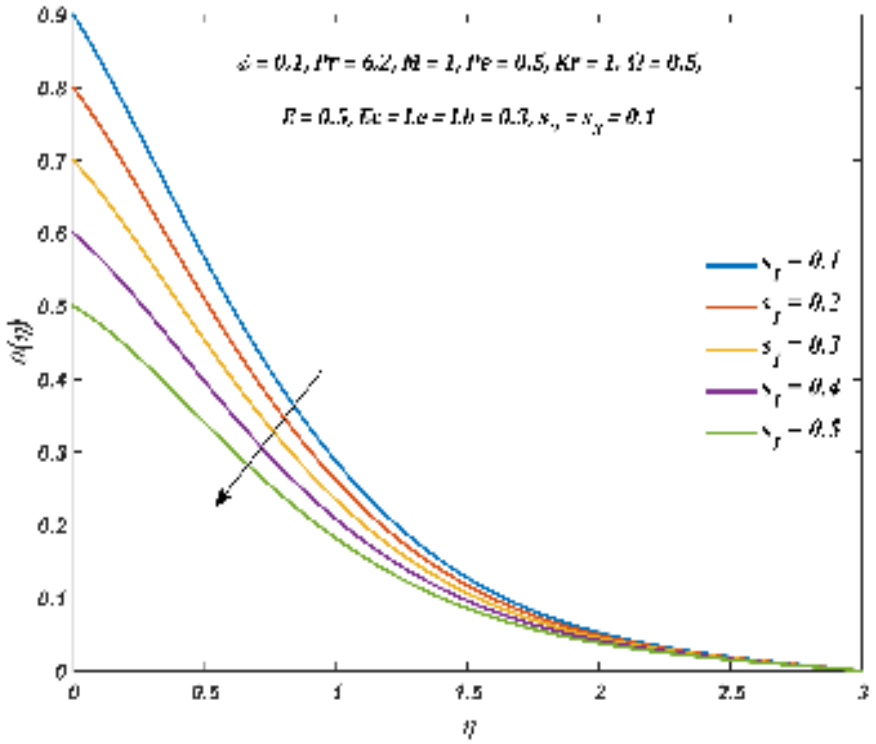

Figure 6.6: $\theta(\eta)$ for differing s_1 values

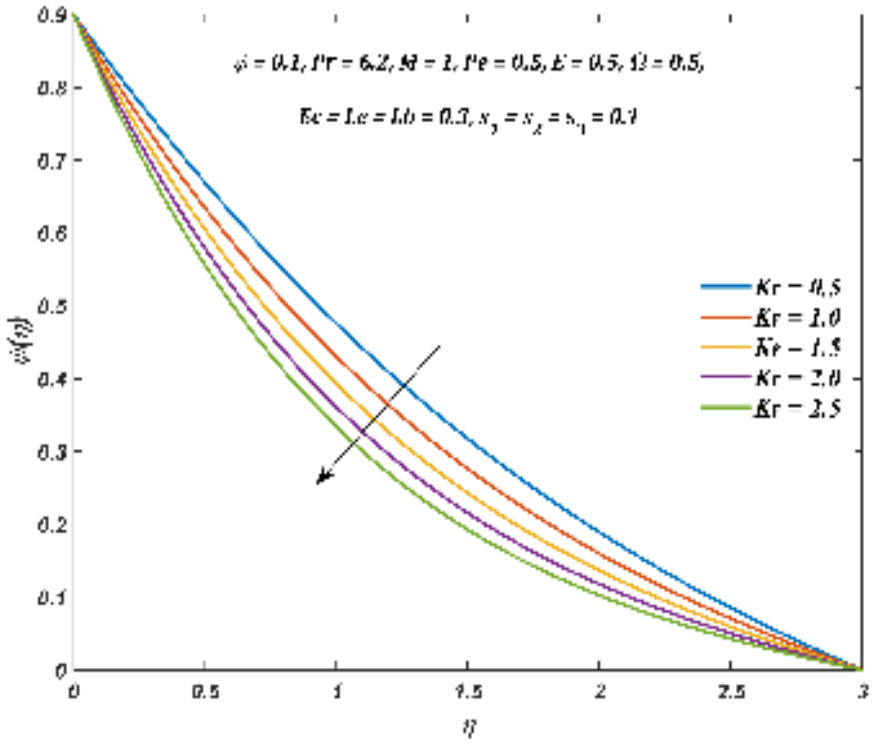

Figure 6.7: $\psi(\eta)$ for differing Kr values

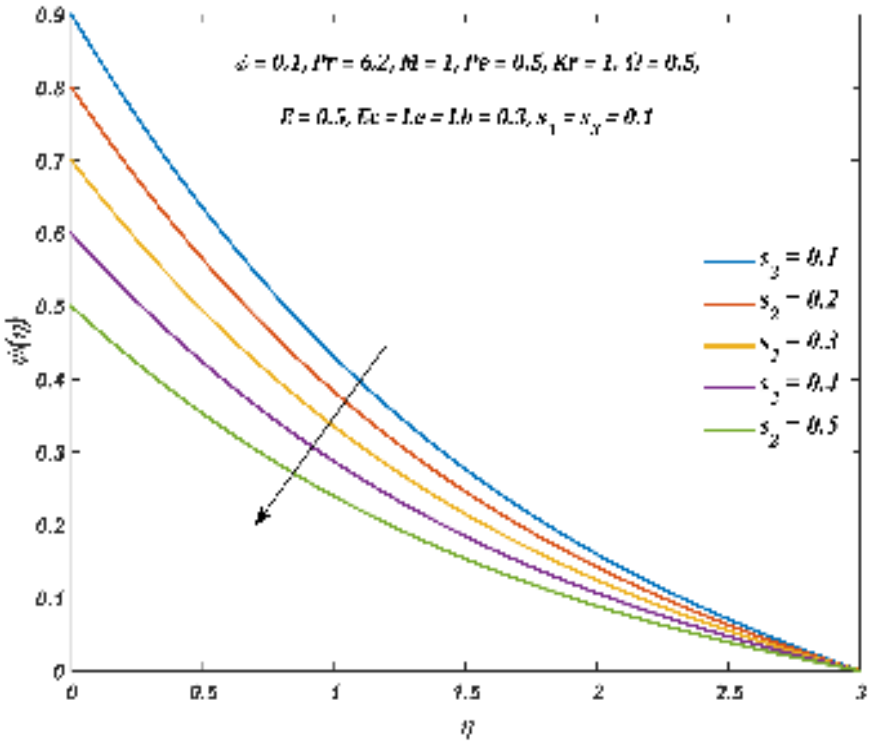

Figure 6.8: $\psi(\eta)$ for differing s_2 values

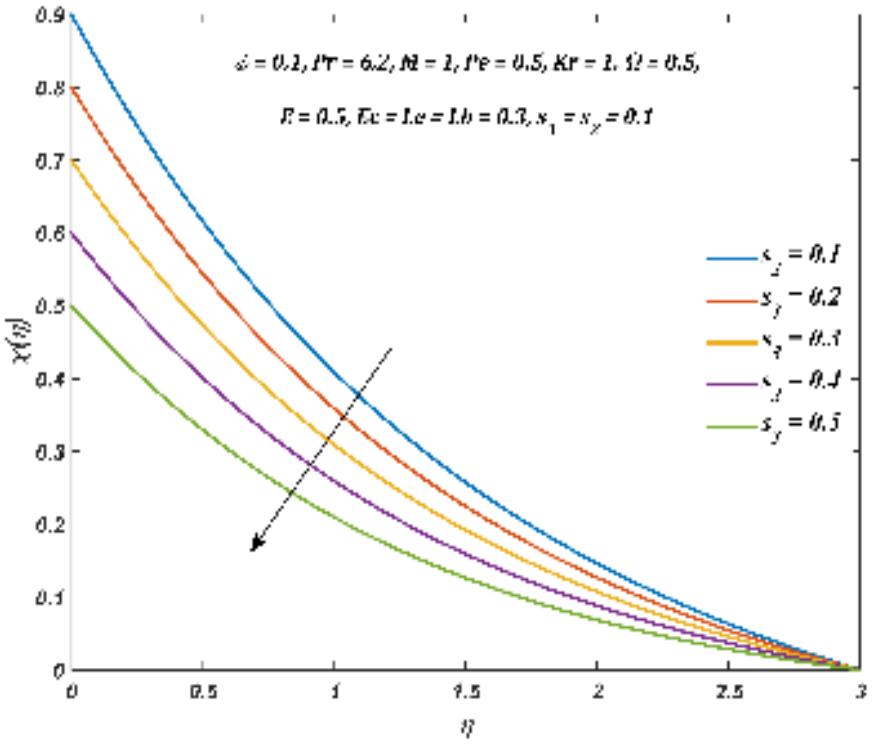

Figure 6.9: $\chi(\eta)$ for differing s_3 values

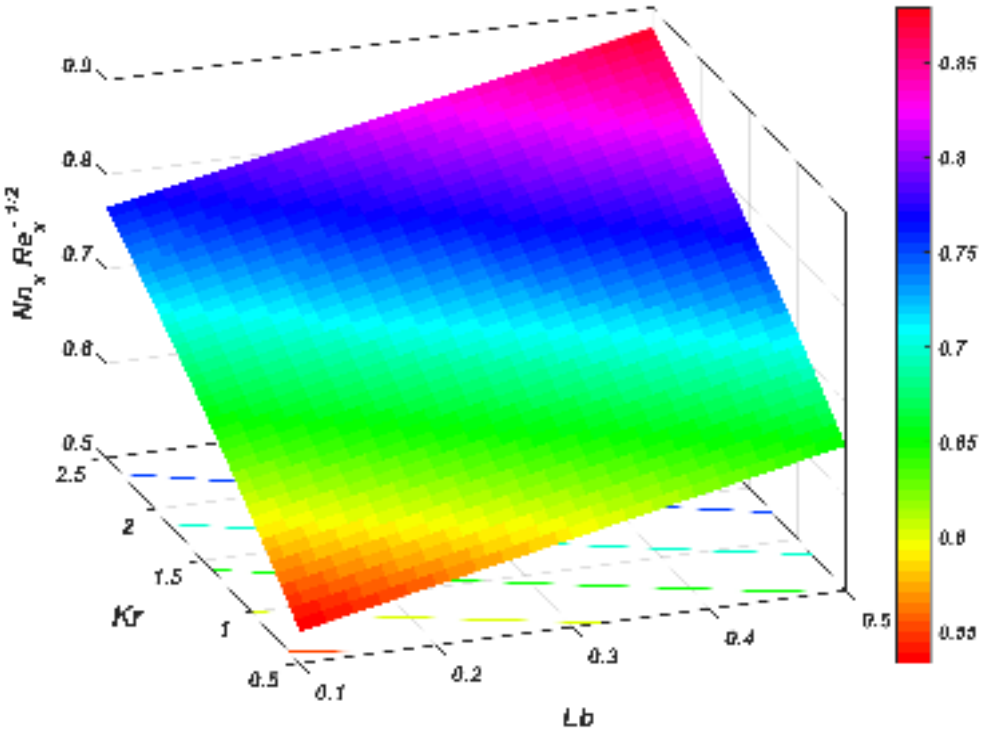

Figure 6.10: Variation of $Nn_x\ Re_x^{-1/2}$ with Kr & Lb

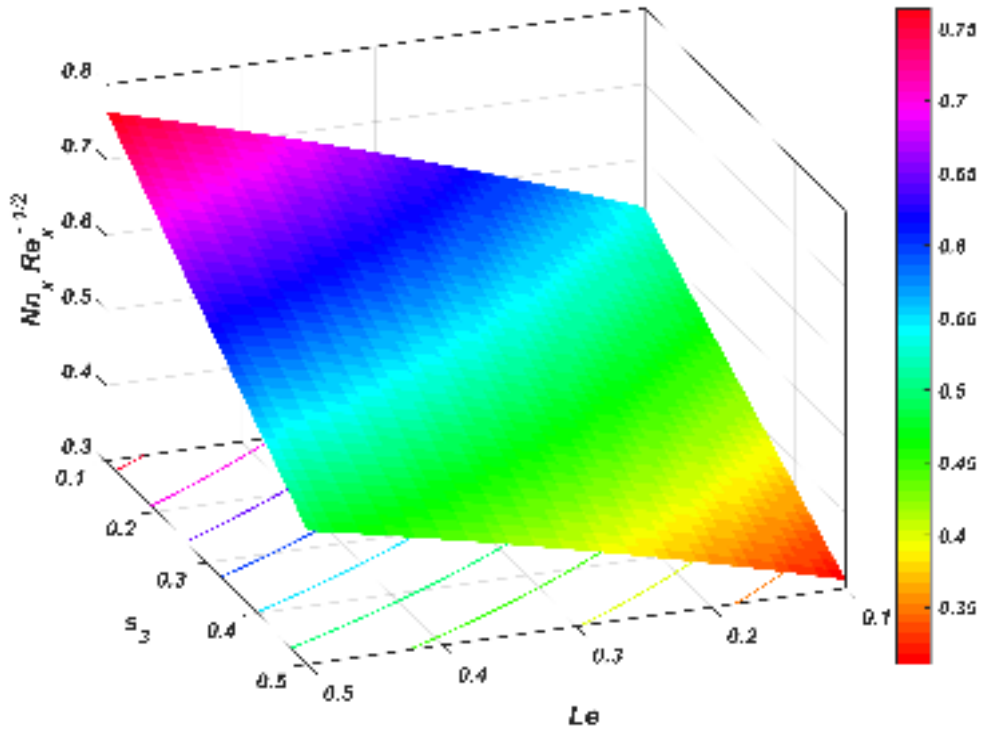

Figure 6.11: Variation of $Nn_x\ Re_x^{-1/2}$ with s_3 & Le

Figures 6.10 & 6.11 explain the simultaneous impact of parameters on microorganism density number. It can be summarised that microorganism density number intensifies with chemical reaction parameter (Kr), Lewis number (Le) & bioconvection Lewis number (Lb). Also, it is perceived that microorganism density number attenuates with motile density stratification parameter (s_3).

Table 6.3: Variation in $Cf_x\ Re_x^{1/2}$ when $Kr = 1,\ Ec = Le = Lb = 0.3,\ Pe = \Omega = 0.5$ & $s_1 = s_2 = s_3 = 0.1$

ϕ	**M**	**E**	$\mathbf{Cf_x\ Re_x^{1/2}}$
0.1	1	0.2	-1.6045
0.1	1	0.4	-1.4112
0.1	1	0.6	-1.2231
0.1	1	0.8	-1.0393
0.1	1	1	-0.8595
Slope			**0.93095**
0.1	0.5	0.5	-1.2699
0.1	1	0.5	-1.3165
0.1	1.5	0.5	-1.3742
0.1	2	0.5	-1.4362
0.1	2.5	0.5	-1.4998
Slope			**-0.1159**
0.02	1	0.5	-1.1016
0.04	1	0.5	-1.1513
0.06	1	0.5	-1.2035
0.08	1	0.5	-1.2585
0.1	1	0.5	-1.3165
Slope			**-2.685**

Table 6.4: Variation in $Nu_x\ Re_x^{-\ 1/2}$ when $Kr = 1,\ Le = Lb = 0.3,\ Pe = \Omega = 0.5$ & $s_2 = s_3 = 0.1$

$\mathbf{s_1}$	ϕ	**Ec**	**M**	**E**	$\mathbf{Nu_x\ Re_x^{-1/2}}$
0.1	0.1	0.3	1	0.2	1.2128
0.1	0.1	0.3	1	0.4	1.5408
0.1	0.1	0.3	1	0.6	1.8084
0.1	0.1	0.3	1	0.8	2.0268
0.1	0.1	0.3	1	1	2.2038
Slope					**1.234**
0.1	0.1	0.3	0.3	0.5	1.5837
0.1	0.1	0.3	0.6	0.5	1.6416
0.1	0.1	0.3	0.9	0.5	1.6743
0.1	0.1	0.3	1.2	0.5	1.6914
0.1	0.1	0.3	1.5	0.5	1.6983
Slope					**0.093**
0.1	0.1	0.1	1	0.5	2.1958
0.1	0.1	0.2	1	0.5	1.9386
0.1	0.1	0.3	1	0.5	1.6814
0.1	0.1	0.4	1	0.5	1.4242
0.1	0.1	0.5	1	0.5	1.167
Slope					**-2.572**
0.1	0.02	0.3	1	0.5	1.2251
0.1	0.04	0.3	1	0.5	1.3626
0.1	0.06	0.3	1	0.5	1.4812
0.1	0.08	0.3	1	0.5	1.5861
0.1	0.1	0.3	1	0.5	1.6814
Slope					**5.6805**
0.1	0.1	0.3	1	0.5	1.6814
0.2	0.1	0.3	1	0.5	1.4088
0.3	0.1	0.3	1	0.5	1.1363
0.4	0.1	0.3	1	0.5	0.8637
0.5	0.1	0.3	1	0.5	0.5912
Slope					**-2.7255**

Table 6.5: Variation in $Sh_x\ Re_x^{-\ 1/2}$ when $M = 1,\ Ec = Lb = 0.3,\ Pe = \Omega = 0.5$ & $s_1 = s_3 = 0.1$

$\mathbf{s_2}$	ϕ	**Kr**	**Le**	**E**	$\mathbf{Sh_x\ Re_x^{-1/2}}$
0.1	0.1	1	0.3	0.2	0.5895
0.1	0.1	1	0.3	0.4	0.5946
0.1	0.1	1	0.3	0.6	0.5994
0.1	0.1	1	0.3	0.8	0.604
0.1	0.1	1	0.3	1	0.6084
Slope					**0.0236**
0.1	0.1	1	0.1	0.5	0.4098
0.1	0.1	1	0.2	0.5	0.508
0.1	0.1	1	0.3	0.5	0.597
0.1	0.1	1	0.4	0.5	0.6785
0.1	0.1	1	0.5	0.5	0.7539
Slope					**0.8587**
0.1	0.1	0.5	0.3	0.5	0.4973
0.1	0.1	1	0.3	0.5	0.597
0.1	0.1	1.5	0.3	0.5	0.6858
0.1	0.1	2	0.3	0.5	0.7663
0.1	0.1	2.5	0.3	0.5	0.8402
Slope					**0.17102**
0.1	0.02	1	0.3	0.5	0.5961
0.1	0.04	1	0.3	0.5	0.5963
0.1	0.06	1	0.3	0.5	0.5965
0.1	0.08	1	0.3	0.5	0.5968
0.1	0.1	1	0.3	0.5	0.597
Slope					**0.0115**
0.1	0.1	1	0.3	0.5	0.597
0.2	0.1	1	0.3	0.5	0.5307
0.3	0.1	1	0.3	0.5	0.4643
0.4	0.1	1	0.3	0.5	0.398
0.5	0.1	1	0.3	0.5	0.3317
Slope					**-0.6633**

Tables 6.3 - 6.5 elucidate the variation of pertinent parameters on drag coefficient, heat transfer and mass transfer rate, respectively. The slope of linear regression (or simply slope) indicates the nature of variation of drag coefficient/heat transfer rate/mass transfer rate. A negative slope implies that the varying parameter has a negative effect on the considered physical quantity. The rate of increase/decrease of physical quantity per unit value of the varying parameter is explained using the slope's magnitude. The main outcomes drawn from Tables 6.3 - 6.5 are:

- The drag coefficient is a decreasing function of M & ϕ and an increasing function of E.
- Mass transfer rate is an increasing function of $E,\ Kr,\ Le$, & ϕ and a decreasing function of s_2.
- Heat transfer rate is a decreasing function of Ec & s_1 and an increasing function of $E,\ M$, & ϕ.

6.5 Statistical Frame

Statistical techniques (like correlation and regression) are largely used by researchers to discover the nature of impact of independent variables (various parameters) on the dependent variable (physical quantities like heat transfer rate/ drag coefficient/ mass transfer rate). Regression analysis aids in quantifying the variation of dependent variable initiated by the change in independent variables. Regression analysis rules out the need for resolving the problem frequently and hence eases the calculation process. For a chosen range of independent variables, an approximate value of the dependent variable can be faultlessly predicted utilizing multiple linear regression.

6.5.1 Correlation and Probable Error

The degree of relationship between two variables is determined with the help of correlation. The sign of correlation coefficient (r) comments on the nature of the relationship while the magnitude of r bespeaks on the dimension of relationship. The positive value of r indicates that an augmentation in the independent variable will beget an improvement in the dependent variable and the negative value of correlation coefficient implies that an augmentation in the independent variable will lower the dependent variable. The reliability of the calculated correlation coefficient

values is guaranteed using probable error (PE). Correlation is said to be significant if $\left|\frac{r}{PE}\right| > 6$; where $PE = \left(\frac{1-r^2}{\sqrt{n}}\right)$ 0.6745 and n is the number of observations [see (Fisher, 1921)].

Table 6.6: Correlation Coefficient (r), Probable Error (PE) and $\left|\frac{r}{PE}\right|$ of drag coefficient

Parameter	**r**	**PE**	$\left\|\frac{\mathbf{r}}{\mathbf{PE}}\right\|$
ϕ	-0.99953	0.000281	3554.453
M	-0.99831	0.001021	977.8618
E	0.999899	6.10E-05	16389.83

Table 6.7: Correlation Coefficient (r), Probable Error (PE) and $\left|\frac{r}{PE}\right|$ of heat transfer rate

Parameter	**r**	**PE**	$\left\|\frac{\mathbf{r}}{\mathbf{PE}}\right\|$
ϕ	0.997314	0.001618	616.3864
Ec	-1	-1.30E-16	7.47E+15
M	0.940793	0.034662	27.14199
E	0.992816	0.004318	229.9108
$\mathbf{s_1}$	-1	1.22E-09	8.21E+08

From Tables 6.6 & 6.7, it is inferred that $Cf_x\ Re_x^{1/2}$ is negatively correlated with M & ϕ and positively correlated with E. Also, it is inferred that $Nu_x\ Re_x^{-1/2}$ is negatively correlated with Ec & s_1 and positively correlated with E, M & ϕ. Further, it is noted that the above results are in good agreement with the numerical results observed in Tables 6.3 & 6.4. Using $\left|\frac{r}{PE}\right|$ values, it can be deduced that all parameters of $Cf_x\ Re_x^{1/2}$ & $Nu_x\ Re_x^{-1/2}$ are significant.

6.5.2 Multiple Linear Regression

Regression analysis is a statistical modelling technique used to establish a relationship between a dependent (drag coefficient or heat transfer rate) and one or more independent (various parameters considered) variables. Since all correlations are significant, multiple linear regression is employed in estimating the drag coefficient and heat transfer rates.

The estimated models are:

$$Cf_{est} = a_\phi \phi + a_M M + a_E E + b$$
$$Nu_{est} = a_\phi \phi + a_M M + a_E E + a_{Ec} Ec + a_{s_1} s_1 + b$$

where $a_\phi,\ a_M,\ a_E,\ a_{Ec},\ a_{s_1}$, and b are the estimated regression coefficients.

Jenkins et al., 2020 elucidated that a sample size of 25 or above would be considered optimal for research based on regressions or meta-regressions. Accordingly, the drag coefficient is estimated from 30 sets of values chosen in the range $[0.02, 0.1]$ for ϕ, $[0.5, 2.5]$ for M & $[0.2, 1]$ for E, and the regression coefficients are calculated using Microsoft Excel. Furthermore, heat transfer rate is also estimated from 30 sets of values chosen in the range $[0.02, 0.1]$ for ϕ, $[0.3, 1.5]$ for M, $[0.2, 1]$ for E, $[0.2, 0.4]$ for Ec, & $[0.1, 0.5]$ for s_1 and the regression coefficients are calculated using Microsoft Excel. Since the p-values for all physical parameters are less than 0.05 the regression coefficients are significant. A negative regression coefficient implies that drag coefficient or heat transfer rate decreases for the corresponding parameter and a positive regression coefficient represents that the corresponding parameter has an increasing effect on drag coefficient or heat transfer rate. The estimated regression models are given below:

$$Cf_{est} = -2.765014142\ \phi - 0.107916023\ M + 0.873312541\ E - 1.370390154$$
$$Nu_{est} = 5.276108658\ \phi + 0.094619221\ M + 1.194981645\ E$$
$$- 2.5720\ Ec - 2.688355065\ s_1 + 1.490951117$$

It is conclusive that E has a positive impact whereas M & ϕ have a negative impact on the drag coefficient. It can also be deduced that E, M, & ϕ have a positive impact while Ec & s_1 descends the heat transfer rate. This is in harmony with the results seen in Tables 6.3 & 6.4.

The original data $\left(Cf_x\ Re_x^{1/2}\ \&\ Nu_x\ Re_x^{-1/2} \right)$ are numerically calculated considering 30 sets of parameter values in the considered range and the estimated data are computed with the aid of estimated regression models (Cf_{est} & Nu_{est}) for the same set of parameter values. Comparison of the estimated data with the original data has been illustrated in Figures 6.12 & 6.13. It is observed that the estimated regression model is capable of predicting the values of drag coefficient and heat transfer rate faultlessly.

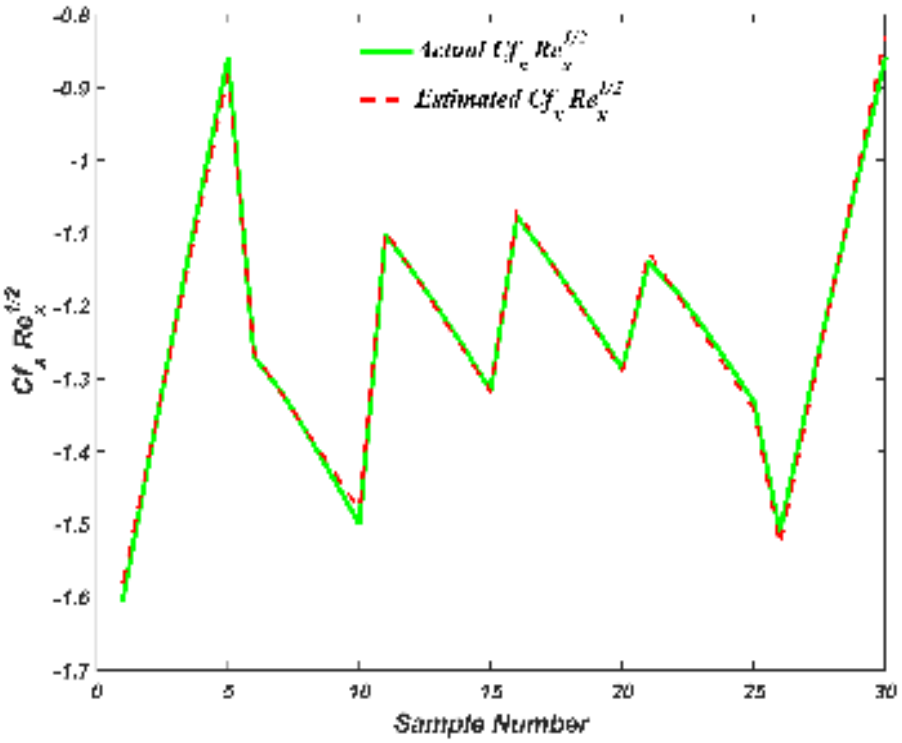

Figure 6.12: Actual versus Estimated $Cf_x\ Re_x^{1/2}$

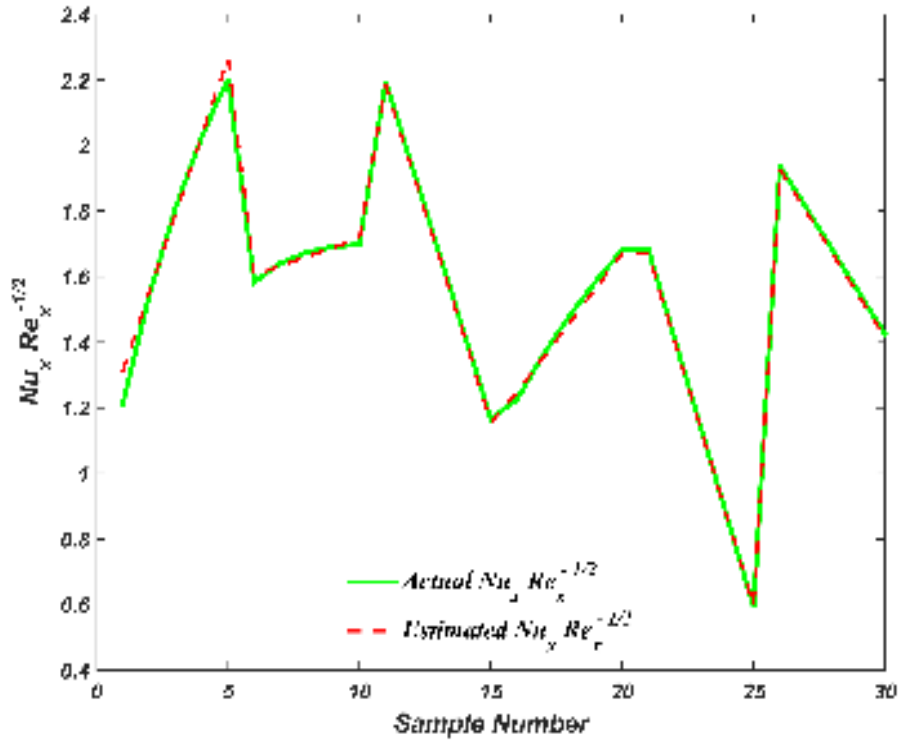

Figure 6.13: Actual versus Estimated $Nu_x\ Re_x^{-1/2}$

6.6 Conclusion

Due to its applications in targeted drug delivery, biomedical imaging, and cancer therapy, the significance of electric and magnetic fields acting on the bioconvective flow considering stratification effects has been examined. The effect of influential parameters on the water-based SWCNT nanofluid flow profiles has been numerically investigated with the aid of the bvp5c scheme. Further, the influence of pertinent parameters on the heat transfer rate and the drag coefficient has been scrutinized utilizing multiple linear regression. In future, the present work can be extended by conducting a detailed theoretical study with more advantageous effects or by considering non-Newtonian fluids. The key points of the present study are:

- Augmenting nanoparticle volume intensifies the nanofluid temperature. This unveils that the nanofluid can be used for killing tumors or cancerous cells.
- Thermal, solutal and motile density stratification parameters exhibit a negative impact on temperature, concentration and microbial concentration, respectively.
- Descending electric field parameter and ascending magnetic field parameter retards the velocity profile, which helps in improving the efficiency of targeted drug delivery and biomedical imaging.
- Microorganism density number is a decreasing function of motile density stratification parameter and an increasing function of chemical reaction parameter.
- The estimated model for drag coefficient, using multiple linear regression, is given by:

$$Cf_{est} = -2.765014142\ \phi - 0.107916023\ M + 0.873312541\ E - 1.370390154$$

- The estimated model for heat transfer rate, using multiple linear regression, is given by:

$$\begin{aligned} Nu_{est} = {} & 5.276108658\ \phi + 0.094619221\ M + 1.194981645\ E \\ & - 2.5720\ Ec - 2.688355065\ s_1 + 1.490951117 \end{aligned}$$

Appendix I: Non-dimensional qunatities

$M = \frac{\sigma_f \ {B_0}^2}{c \ \rho_f}$	Magnetic field parameter
$E = \frac{E_0}{B_0 \ U_W}$	Electric field parameter
$Pr = \frac{(\mu C_p)_f}{k_f} = \frac{\vartheta_f}{\alpha_f}$	Prandtl number
$Kr = \frac{k_r}{c}$	Chemical reaction parameter
$Ec = \frac{(cx)^2}{(C_p)_f (T_W - T_0)}$	Eckert number
$Le = \frac{\vartheta_f}{D_B}$	Lewis number
$Lb = \frac{\vartheta_f}{D_m}$	Bioconvection Lewis number
$Pe = \frac{bW_c}{D_m}$	Bioconvection Peclet number
$\Omega = \frac{N_\infty}{N_W - N_0}$	Microorganism concentration difference parameter
$s_1 = \frac{\delta_2}{\delta_1}$	Thermal stratification parameter
$s_2 = \frac{\epsilon_2}{\epsilon_1}$	Solutal stratification parameter
$s_3 = \frac{\xi_2}{\xi_1}$	Motile density stratification parameter

Appendix II: Nomenclature

c	Dimensional constant	W_c	Maximum cell swimming speed
u, v	Velocity components	B_0	Uniform magnetic field
Nn_x	Local motile density	T_∞	Ambient fluid temperature
T_0	Reference temperature	N_∞	Ambient microbial concentration
C	Fluid concentration	C_0	Reference nanoparticle concentration
T	Fluid temperature	N_0	Reference microbial concentration
x, y	Cartesian coordinates	N_w	Microbial concentration near wall
b	Chemotaxis constant	C_w	Nanoparticle concentration near wall
T_w	Wall fluid temperature	C_∞	Ambient nanoparticle concentration
C_p	Specific heat	Cf_x	Local drag coefficient
k_r	Reaction rate constant	Nu_x	Local Nusselt number
Sh_x	Local Sherwood number	N	Microorganism concentration
σ	Electrical conductivity	E_0	Uniform electric field
η	Dimensionless variable	D_B	Chemical molecular diffusivity
ϑ	Kinematic viscosity	D_m	Microorganism diffusion coefficient
k	Thermal conductivity	Ω	Microorganism concentration difference
α	Thermal diffusivity		parameter
ρ	Fluid density	ϕ	Nanoparticle volume fraction